Thermal Oxidation Kinetics for a Poly(bismaleimide)

X. COLIN,[1,2] C. MARAIS,[1] J. VERDU[2]

[1] ONERA, Département Matériaux et Systèmes Composites, 29 avenue de la Division Leclerc, 92322 Châtillon Cedex, France

[2] ENSAM, Laboratoire de Transformation et de Vieillissement des Polymères, 151 boulevard de l'Hôpital, 75013 Paris, France

Received 16 November 2000; accepted 6 February 2001

ABSTRACT: The thermal oxidation of poly(bismaleimide) of the F655-2 type, supplied by Hexcel-Genin, was studied by isothermal gravimetry at 180, 210, and 240°C and various oxygen pressures ranging from 0 to 1.2 bar. Comparison of various sample thicknesses and visible microscopy observations on bulk aged samples shows that the whole oxidized layer has a depth of about 75 μm at 240°C, 138 μm at 210°C, and 229 μm at 180°C. An attempt was made to build a kinetic model to predict this depth. It is based on a differential equation in which O_2 diffusion and its consumption rate, $r(C)$, are coupled, C being the O_2 concentration. Its resolution needs two sets of experiments: the first one to determine the O_2 diffusivity and solubility in the polymer, and the second one to determine $r(C)$. The mathematical form of $r(C)$ is derived from a mechanistic scheme of radical chain oxidation in which initiation is mainly due to POOH decomposition. This expression contains two kinetic parameters, α and β, the values of which are determined from the experimental curves of mass loss rate against O_2 pressure (in the stationary state). The theoretical predictions, at each temperature under consideration, are in excellent agreement with experimental results. © 2001 John Wiley & Sons, Inc. J Appl Polym Sci 82: 3418–3430, 2001

Key words: poly(bismaleimide); oxidation; kinetics; diffusion control; oxidized layer

INTRODUCTION

Some peculiarities of the behavior of thermostable polymers at a moderate temperature (typically below 250°C), in neutral atmosphere, could be explained by the following (oversimplified) mechanistic scheme:

(Ta) P—P (polymer) $\rightarrow$ [P° P°]$_{cage}$ (k_i)
thermolysis into caged radicals

(Tb) [P° P°]$_{cage}$ $\rightarrow$ P—P (k_R)
recombination

(Tc) [P° P°]$_{cage}$ $\rightarrow$ 2P° (k_D)
diffusion of radicals out of cage

At low conversions, k_i[P—P] = $r_i \approx$ constant. By using a stationary state assumption, we can determine the rate of radical build-up:

$$\frac{d[P^\circ]}{dt} = 2r_i \frac{k_D}{k_R + k_D}[1 - \exp(-(k_R + k_D)t)] \quad (1)$$

In the case under study (thermostable polymers in glassy state), one can see two causes of stability:

(i) Because the main rule of chemical design of thermostable polymers is "avoid bonds of low dissociation energy," the rate r_i of dissociation of P—P bonds is expected to be relatively low.

Correspondence to: J. Verdu (ltvp@paris.ensam.fr).

Journal of Applied Polymer Science, Vol. 82, 3418–3430 (2001)

(ii) Because the polymer is in its glassy state (in common use conditions), the molecular mobility is low and thus, cage recombination of radical pairs is favored ($k_D/(k_R + k_D) \ll 1$).

Thus, the probability of radical formation, which results from the combination of two events of relatively low probability, bond dissociation and escape of primary radicals from the cage, is expected to be very low.

In the presence of O_2, however, the situation becomes completely different for the following reasons:

(i) Oxidation propagates by O_2 addition to radicals (very fast) and hydrogen abstraction:

$$\text{(II)} \quad P^\circ + O_2 \rightarrow PO_2^\circ \quad (k_2)$$

$$\text{(III)} \quad PO_2^\circ + PH \rightarrow PO_2H + P^\circ \quad (k_3)$$

Above 180°C, PO_2° radicals are sufficiently reactive to abstract hydrogens on relatively thermostable CH bonds, for instance, methyl or, even, aryls.

(ii) As soon as hydroperoxides are formed, they become the main source of radicals owing to their very low dissociation energy: E_D[—O—O—] $\approx$ 150 kJ mol^{-1} against $E_D \geq$ 450 kJ mol^{-1} for most of the other polymer bonds. Then, the hydroperoxide decomposition rapidly becomes the largely predominant initiation process in chain oxidation at moderate temperature in the glassy state of thermostable polymers.

These remarks justify the use of a closed loop mechanism scheme[1] in which oxidation generates its own initiator, POOH, radical formation by polymer thermolysis being negligible. The purpose of this article is to try to build a kinetic model, derived from this scheme and coupled with O_2 diffusion equation to predict the thickness distribution of oxidation products, minimizing the number of empirical steps. Knowledge of the oxidation thickness gradients is necessary to predict the mechanical behavior (spontaneous cracking induced by density gradients resulting from oxidation). The strategy of investigation is summarized in Figure 1. We start from three sets of experiments:

Set 1: Oxidation at various temperatures and O_2 pressures of sufficiently thin samples having an almost homogeneous degradation within the thickness. The main aging function here is the mass change, which is linked to the oxidation rate through a simple but checkable hypothesis.

Set 2: Permeation experiments to obtain the solubility and diffusivity of O_2 into the polymer.

Set 3: Oxidation at atmospheric pressure of samples of various thicknesses to determine experimentally the thickness of the oxidized layer and to check the theoretical predictions.

The closed loop mechanistic scheme is used to establish the relationship between O_2 consumption rate, $r(C)$, and the O_2 concentration, C, into the polymer. The main parameters of this relationship are determined from gravimetric data. Then, the now classical diffusion/reaction equation[2] is used to predict the thickness distribution of O_2 concentration:

$$\frac{\partial C}{\partial t} = D \frac{\partial^2 C}{\partial x^2} - r(C) \tag{2}$$

where D is the O_2 coefficient of diffusion and x is the layer abscissa in the sample thickness, the boundary conditions being $C = 0$ at every depth of $t = 0$, and $C = C_S$ at $x = +L/2$ and $x = -L/2$ every time. C_S is the equilibrium O_2 concentration in the polymer, which is given by the Henry's law in a function of the O_2 coefficient of solubility, S, and the O_2 partial pressure, p: $C_S = Sp$, and L is the sample thickness (the origin of x is taken in the middle of the sample).

EXPERIMENTAL

Materials

The polymer matrix was selected for this study after a previous assessment of the oxidative stability of fiber/resin systems currently used in aircraft composite structures.[3] It is a poly(bismaleimide) matrix of F655-2 type provided by Hexcel-Genin.

F655-2 films and plates were processed by press-molding and then postcured under primary vacuum in accordance with the recommended cure cycle. Prior to testing, all the materials were inspected by physical means. Particularly, the

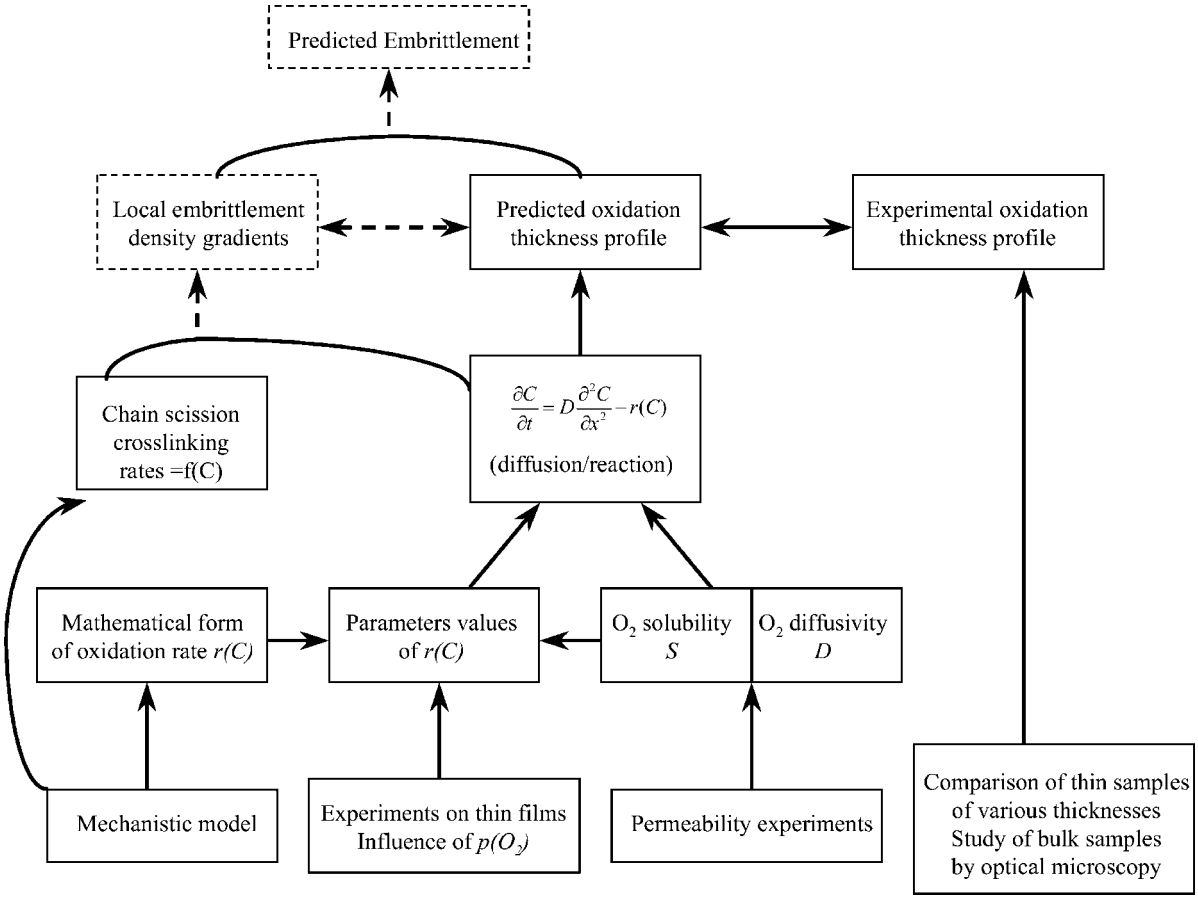

Figure 1 Scheme showing the strategy for the prediction of the thickness oxidation profile. The parts in dashed lines correspond to future developments to predict embrittlement.

glass transition temperature, T_g, was measured by means of differential scanning calorimetry. Considering T_g as the temperature of the onset of the endothermal increase, a heating rate of 20°C/min gives T_g around 255°C.

Experimental Procedures

All the specimens were put under vacuum (10^{-3} bar) before testing. All the thermal tests were performed below the glass transition temperature of the polymer.

O_2 coefficients of diffusion, D, and solubility, S, were determined experimentally at various temperatures from 20°C up to 120°C. For that, a polymer film is put between two capacities,[4] the first one contains oxygen at 1 bar in pressure, whereas the second one initially is under vacuum (10^{-5} Pa). The pressure difference induces a gas flow through the sample. The gas, which penetrates in the second capacity, is analyzed by means of a mass spectrometer which gives access to the O_2 partial pressure versus time.

The influence of O_2 partial pressure on the chemical reaction kinetics was determined by subjecting very thin polymer films to isothermal aging between 180 and 240°C. The polymer sample is placed on a plateau of a Mettler AM50 microbalance to carry out various N_2/O_2 atmosphere tests until 1.2 bar in pressure. The weight of the sample is continuously recorded versus aging time for each temperature.

The coupling of O_2 diffusion and chemical reactions was investigated by exposing various sample thicknesses to isothermal aging conditions between 180 and 240°C in air-circulating ovens. Most of the samples were removed intermittently from ovens, cooled at room temperature in a dessicator, weighted, and returned to ovens. Other samples were removed at definite aging times and examined by optical microscopy, after polishing of cross sections, by using an interferential contrast.

KINETIC SCHEME

The following mechanistic scheme was chosen:

Initiation	$POOH \rightarrow 2P^\circ + H_2O + \nu Mv$	(k_1)
Propagation	$P^\circ + O_2 \rightarrow PO_2^\circ$	(k_2)
Propagation	$PO_2^\circ + PH \rightarrow PO_2H + P^\circ$	(k_3)
Termination	$P^\circ + P^\circ \rightarrow$ inactive products	(k_4)
Termination	$P^\circ + PO_2^\circ \rightarrow$ inactive products	(k_5)
Termination	$PO_2^\circ + PO_2^\circ \rightarrow$ inactive products + O_2	(k_6)

It is hypothesized that hydroperoxide decomposition is unimolecular, as expected in the high temperature range.[5] The mechanism can in fact be decomposed as follows:

$$\text{(Ia)} \quad POOH \rightarrow PO^\circ + {}^\circ OH$$

$$\text{(Ib)} \quad HO^\circ + PH \rightarrow P^\circ + H_2O$$

$$\text{(Ic)} \quad PO^\circ + PH \rightarrow POH + P^\circ$$

$$\text{(Id)} \quad PO^\circ \rightarrow P{=}O + P^\circ$$

$$\overline{POOH \rightarrow 2P^\circ + H_2O + \alpha POH + (1-\alpha)P{=}O}$$

PO° and $^\circ OH$ radicals are very reactive and thus short-lived. It is assumed that alkyl radicals resulting from the rearrangement of PO° radicals by β scission (Id) are equivalent to the other alkyl radicals resulting from hydrogen abstraction.

It is noteworthy that, in a such scheme, volatile products, if they are formed, can result only from initiation or termination reactions. On the other hand, at high temperature, k_1 is very high and the induction time, which is proportional to the reciprocal of k_1,[1] is expected to be very short so that the system is expected to reach rapidly a stationary state. In these conditions, initiation and termination rates are almost equal and it becomes licit, from the point of view of kinetic modeling, to consider that weight loss comes only from initiation. The average molar mass of volatile fragments would be M_V and their yield would be ν.

A kinetic model can be built from the following set of equations:

$$\frac{d[P^\circ]}{dt} = 2k_1[POOH] - k_2C[P^\circ] + k_3[PH][PO_2^\circ] - 2k_4[P^\circ]^2 - k_5[P^\circ][PO_2^\circ] \quad (3)$$

$$\frac{d[PO_2^\circ]}{dt} = k_2C[P^\circ] - k_3[PH][PO_2^\circ] - k_5[P^\circ][PO_2^\circ] - 2k_6[PO_2^\circ]^2 \quad (4)$$

$$\frac{d[POOH]}{dt} = k_3[PH][PO_2^\circ] - k_1[POOH] \quad (5)$$

$$r(C) = k_2C[P^\circ] - k_6[PO_2^\circ]^2 \quad (6)$$

$$\frac{d[V]}{dt} = \nu k_1[POOH] \quad (\text{in the volatile formation, } \nu \text{ is a stoichiometric parameter}) \quad (7)$$

$$\frac{d[H_2O]}{dt} = k_1[POOH] \quad (8)$$

$$\frac{d(m/m_0)}{dt} = \frac{32}{\rho}\, r(C) - \frac{18}{\rho}\frac{d[H_2O]}{dt} - \frac{M_V}{\rho}\frac{d[V]}{dt} \quad (\rho \text{ is the polymer density}) \quad (9)$$

In the stationary state, the system of eqs. (3), (4), and (5) simplifies to

$$2k_1[POOH] = 2k_4[P^\circ]^2 + 2k_5[P^\circ][PO_2^\circ] + 2k_6[PO_2^\circ]^2 \quad (10)$$

$$k_1[POOH] = k_3[PH][PO_2^\circ] \quad (11)$$

so that

$$k_4[P^\circ]^2 + k_5[P^\circ][PO_2^\circ] - k_3[PH][PO_2^\circ] + k_6[PO_2^\circ]^2 = 0 \quad (12)$$

which leads to

$$[P^\circ] = \frac{k_5[PO_2^\circ]}{2k_4}\left\{-1 + \left[1 + \psi\left(\frac{[PO_2^\circ]_0}{[PO_2^\circ]} - 1\right)\right]^{1/2}\right\} \tag{13}$$

where

$$\psi = \frac{4k_4k_6}{k_5^2} \quad \text{and} \quad [PO_2^\circ]_0 = \frac{k_3[PH]}{k_6}.$$

$[PO_2^\circ]_0$ is the maximum possible PO_2° concentration in O_2 excess. As shown by Gillen et al.,[6] $\psi \ll 1$. Thus, in a large interval of $[PO_2^\circ]$ variation, such as typically,

$$\frac{[PO_2^\circ]}{[PO_2^\circ]_0} \gg \frac{5\psi}{1 + 5\psi}$$

one can use the classical approximation to obtain

$$[P^\circ] = \frac{k_5}{k_6}([PO_2^\circ]_0 - [PO_2^\circ]) \tag{14}$$

which gives by substitution in eq. (4):

$$\frac{d[PO_2^\circ]}{dt} = -k_6\left[[PO_2^\circ]^2 + \left(\frac{k_2C}{k_5} + 2[PO_2^\circ]_0\right) \times [PO_2^\circ] - \frac{k_2C}{k_5}[PO_2^\circ]_0\right] \tag{15}$$

The stationary state value is given by the positive root

$$[PO_2^\circ] = \frac{1}{2}\left(\frac{k_2C}{k_5} + 2[PO_2^\circ]_0\right) \times \left\{-1 + \left[1 + \frac{4(k_2C/k_5)[PO_2^\circ]_0}{((k_2C/k_5) + 2[PO_2^\circ]_0)^2}\right]^{1/2}\right\} \tag{16}$$

so that

$$[PO_2^\circ] \approx \frac{(k_2C/k_5)[PO_2^\circ]_0}{(k_2C/k_5) + 2[PO_2^\circ]_0} = [PO_2^\circ]_0\frac{\beta C}{1 + \beta C} \tag{17}$$

where

$$\beta = \frac{k_2k_6}{2k_5k_3[PH]} \tag{18}$$

$[P^\circ]$ can be then determined from eq. (14):

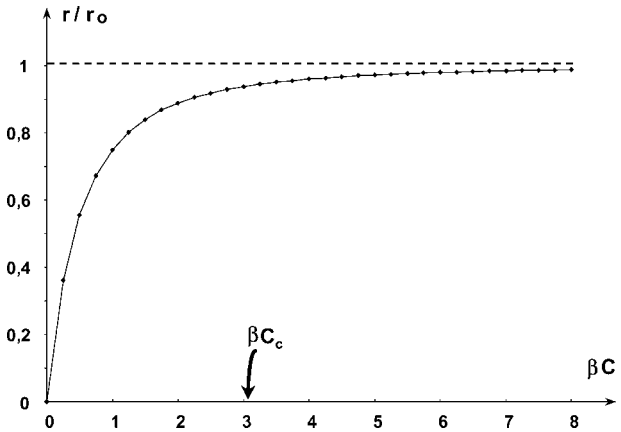

Figure 2 Reduced O_2 consumption rate against reduced O_2 concentration.

$$[P^\circ] = \frac{k_3[PH]}{k_5}\frac{1}{1 + \beta C} \tag{19}$$

From $[P^\circ]$ and $[PO_2^\circ]$, all the important kinetic quantities can be calculated.

For instance, eq. (6) gives

$$r(C) = 2\frac{k_3^2[PH]^2}{k_6}\frac{\beta C}{1 + \beta C}\left[1 - \frac{\beta C}{2(1 + \beta C)}\right] \tag{20}$$

which leads to $C \to \infty$,

$$r(C) \to r_0 = \frac{k_3^2[PH]^2}{k_6}$$

and eq. (20) can be rewritten as:

$$r(C) = 2r_0\frac{\beta C}{1 + \beta C}\left[1 - \frac{\beta C}{2(1 + \beta C)}\right] \tag{21}$$

One can then plot the curve into reduced coordinates

$$\frac{r}{r_0} = f(\beta C)$$

(see Fig. 2). One can reasonably consider that the O_2 consumption rate reaches its saturation level, r_0, when $\beta C \geq 3$, for example,

$$C \geq C_C \quad \text{with} \quad C_C \approx 6\frac{k_5}{k_2}\frac{k_3[PH]}{k_6} \tag{22}$$

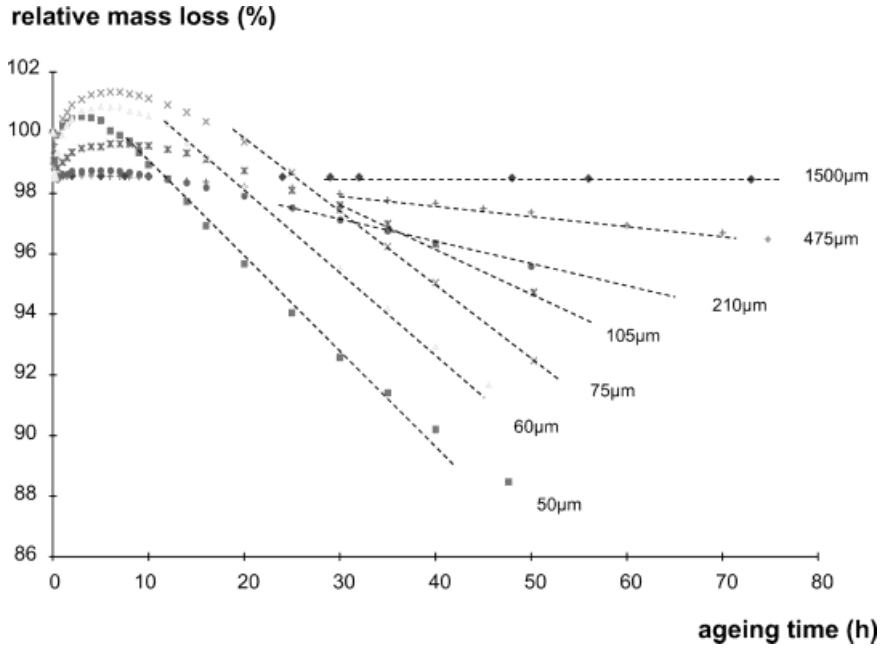

Figure 3 Example of gravimetric curves obtained for various sample thicknesses in air at 240°C. [Color figure can be viewed in the online issue, which is available at www.interscience.wiley.com.]

The POOH equilibrium concentration is given by eq. (5):

$$[\mathrm{POOH}] = \frac{k_3[\mathrm{PH}]}{k_1}[\mathrm{PO}_2^\circ] = \frac{k_3^2[\mathrm{PH}]^2}{k_1 k_6}\frac{\beta C}{1+\beta C} \quad (23)$$

Then, the mass variation in stationary state can be determined from eq. (9):

$$\frac{d(m/m_0)}{dt} = \frac{64}{\rho}\frac{k_3^2[\mathrm{PH}]^2}{k_6}\frac{\beta C}{1+\beta C}\left[1 - \frac{\beta C}{2(1+\beta C)}\right] - \frac{(18+\nu M_V)}{\rho}\frac{k_3^2[\mathrm{PH}]^2}{k_6}\frac{\beta C}{1+\beta C}$$

so that

$$\frac{d(m/m_0)}{dt} = \frac{1}{\rho}\frac{\alpha C}{1+\beta C}\left[(46-\nu M_V) - \frac{32\beta C}{1+\beta C}\right] \quad (24)$$

where

$$\alpha = \frac{k_2 k_3[\mathrm{PH}]}{2k_5} \quad (25)$$

For example, in oxygen excess ($C \to \infty$):

$$\left(\frac{d(m/m_0)}{dt}\right)_0 = \frac{1}{\rho}\frac{\alpha}{\beta}(14-\nu M_V) \quad (26)$$

Finally, if the oxygen concentration profiles are known, the mass variation of a bulk specimen can be computed by using eq. (24) and the relation:

$$\frac{d(M/M_0)}{dt} = \frac{2}{L}\int_0^L \frac{d(m/m_0)}{dt}\,dx \quad (27)$$

RESULTS

Determination of the Critical Thickness for Diffusion Control

Samples of BMI network of various thicknesses ranging from 50 to 1500 μm were exposed at 240°C in air. The corresponding gravimetric curves are shown in Figure 3. The mass increases in the early hours of exposure and then decreases. The mass loss rate tends rapidly toward an almost constant value, indicating the existence of a stationary state. The initial increase results from the closed loop character of the reaction. As a matter of fact, it can be demonstrated that in such a process, the initiation rate increases and the

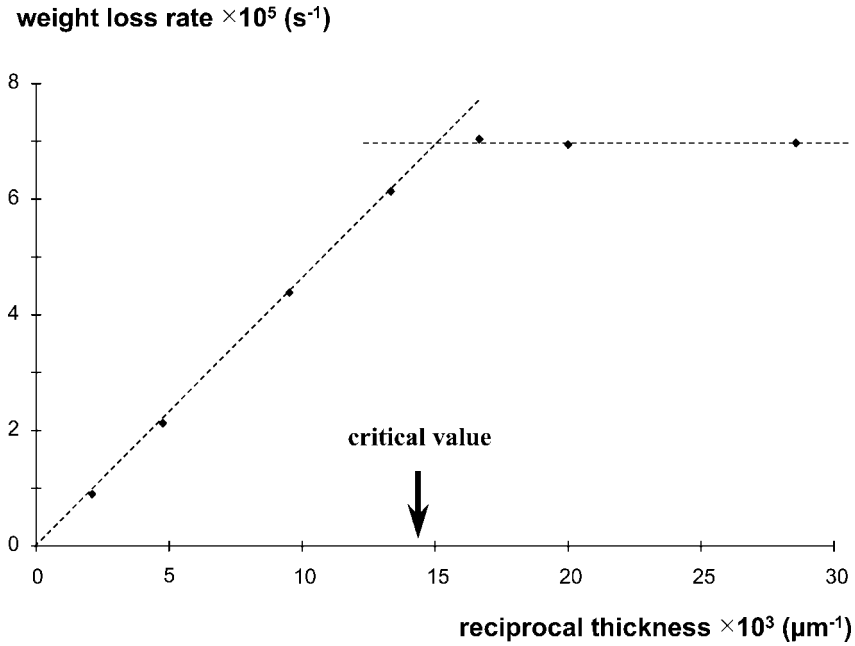

Figure 4 Maximum weight loss rates determined for various sample thicknesses in air at 240°C (in the stationary state).

kinetic chain length decreases with time.[7] Mass increase, due to O_2 incorporation in macromolecules, is essentially linked to propagation, whereas mass loss, as previously shown, occurs only in initiation or termination. It is thus not surprising to find a predominance of mass gain in the early hours and a predominance of mass loss later (when the kinetic chain length tends toward unity). The same behavior was observed, for instance, in the polypropylene thermooxidation.[8]

The stationary rates of mass loss graphically determined in Figure 3 were plotted against the reciprocal of the sample thickness in Figure 4. The existence of two distinct regimes is clearly in evidence. For low thicknesses, typically below 75 μm, the mass loss rate is independent of the thickness. For high thicknesses, it is proportional to the reciprocal of the thickness. This behavior can be easily explained as follows. The thickness of the oxidized layer, l_{ox}, in bulk samples, is independent of the whole sample thickness. There is thus a critical thickness, $L_C = 2l_{ox}$, so that for $L < L_C$, oxidation is homogeneous and independent of thickness, whereas for $L > L_C$, the absolute mass loss rate is proportional to the volume fraction undergoing oxidation (i.e., inversely proportional to the sample thickness). The same experiment was done at various temperatures and gave the critical thickness L_C values listed in Table I.

Determination of Kinetic Parameters of the Nondiffusion Controlled Regime

The experiments were done on a sample with a thickness of 50 μm ($\pm$5 μm), well below the critical value, to avoid heterogeneities due to O_2 diffusion control. The gravimetric curves were recorded in isothermal conditions at various O_2 pressures ranging from 0 to 1.2 bar. The shape of the curves obtained at 240°C is shown in Figure 5. The curves display a wide inflexion range corresponding (see the Discussion) to the stationary state. For each O_2 partial pressure, oxygen concentration within the film was calculated by using the Henry's law and the measured solubility coefficient, S,

$$C = Sp \quad \text{with} \quad S = 3.61 \times 10^{-4} \text{ mol m}^{-3} \text{ Pa}^{-1}$$

(independent of temperature)

and the corresponding mass loss rate was determined in the stationary state. Then, weight loss

Table I Critical Values Measured at 240, 210, and 180°C in Air

Aging temperature (°C)	240	210	180
Critical value (μm)	75	100	150

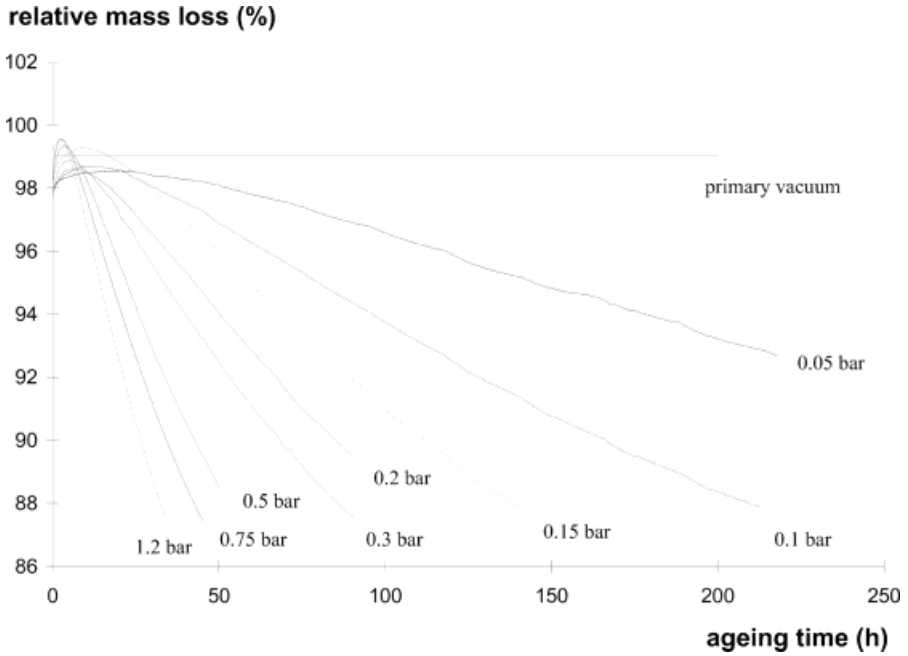

Figure 5 Example of gravimetric curves obtained for 50-μm-thick polymer films at 240°C in various O_2 partial pressures. [Color figure can be viewed in the online issue, which is available at www.interscience.wiley.com.]

rate was plotted against oxygen concentration in Figure 6. These results can be summarized as follows:

(i) There is no measurable mass loss in the absence of O_2, which confirms that mass loss is only due to oxidation and can be

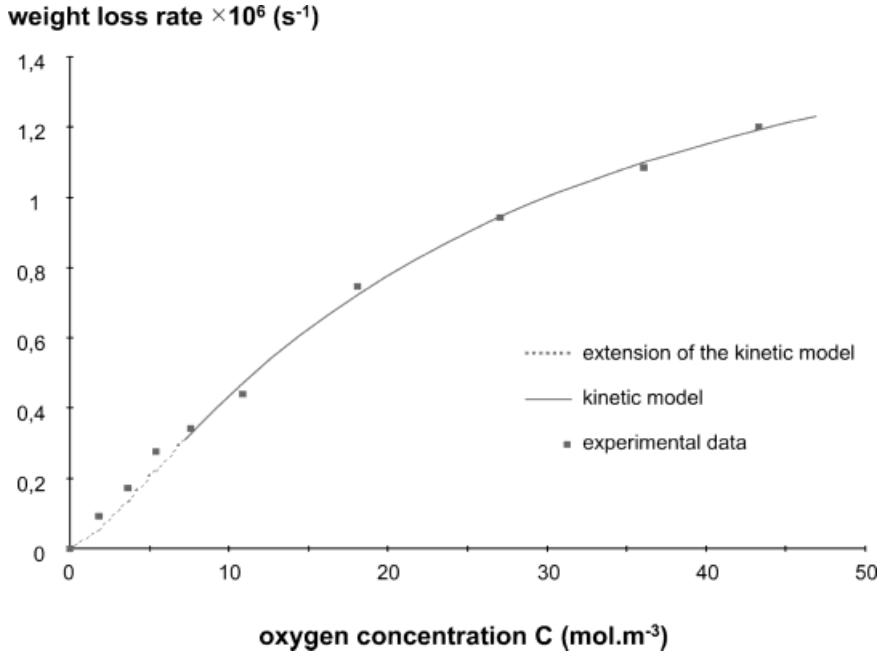

Figure 6 Maximum weight loss rate determined for 50-μm-thick films exposed to various O_2 partial pressures at 240°C (in the stationary state). Comparison with theoretical values calculated with analytical expression (24). [Color figure can be viewed in the online issue, which is available at www.interscience.wiley.com.]

Table II Coefficient Values for Eq. (24) Determined at 240, 210, and 180°C in Air

Aging Temperature (°C)	α (s^{-1})	β (l mol^{-1})	νM_V (g mol^{-1})
240	$(5.3 \pm 3).10^{-3}$	79.4 ± 28.7	50.6 ± 10.6
210	$(1.1 \pm 0.5).10^{-3}$	81.4 ± 23.1	53.2 ± 9.8
180	$(2.5 \pm 0.8).10^{-4}$	61.0 ± 31.7	47.5 ± 10.6

considered as an argument in favor of the closed loop model; initiation by polymer thermolysis can be neglected relative to hydroperoxide decomposition in the temperature range under consideration.

(ii) The curve of Figure 6 displays the expected shape presented in Figure 2.

(iii) The values of parameters α, β, and M_V were determined from eqs. (24) and (26). The results of the experiments made at 240, 210, and 180°C are given in Table II and call for the following comments:

The model well fits the experimental data (see Fig. 6) except eventually at low O_2 concentrations where the starting approximations [eqs. (13) and (14)] are no longer valid. It is, however, difficult to imagine very strong discontinuities of the variations of oxidation rate in this range, so that the proposed model can be considered acceptable in the whole O_2 concentration range.

The value of νM_V, about 50 g mol^{-1}, seems to be physically realistic. Since ν is a yield, in principle lower than unity, this means that the volatile fragments have an average molar mass of at least 50 g mol^{-1}; however, significantly larger fragments would not be released at a rate independent of the thickness, owing to their low diffusivity in glassy state bismaleimide. It is thus reasonable to suppose that mass loss is due to a frequent process ($\nu \approx 1$) giving volatile fragments larger than O_2 molecule but not too much (for instance, CO_2, benzene, etc.).

Thickness Profile of Oxidation Products Concentration (Diffusion Controlled Regime)

Experimental determinations were made on bulk samples exposed at 180, 210, and 240°C in air. After aging, a polished cross section is examined by optical microscopy by using interferential contrast. The oxidized layer appears rougher and brighter than the core (see Fig. 7). One can envisage two distinct criteria to define the skin-core boundary: criterion 1 would correspond to the superficial, brightest zone of thickness about 40 μm in Figure 7, whereas criterion 2 would correspond to the whole zone of visible changes, including an intermediary layer, darker than the superficial one, with an approximate thickness of 35 μm. The corresponding values of both thicknesses of the oxidized layer are reported in Table III.

Equations (2) and (21) were used to predict theoretically the thickness distribution of O_2 concentrations, using the above determined kinetic parameters and diffusivity, D, values such as

$$D = D_0 \exp\left(-\frac{E_D}{RT}\right) \quad \text{with} \quad D_0 = 2.0 \times 10^{-10}\ \text{m}^2\ \text{s}^{-1}$$

and

$$E_D = 16.1\ \text{kJ mol}^{-1}$$

were previously determined in the 20–120°C interval from permeation experiments and then D

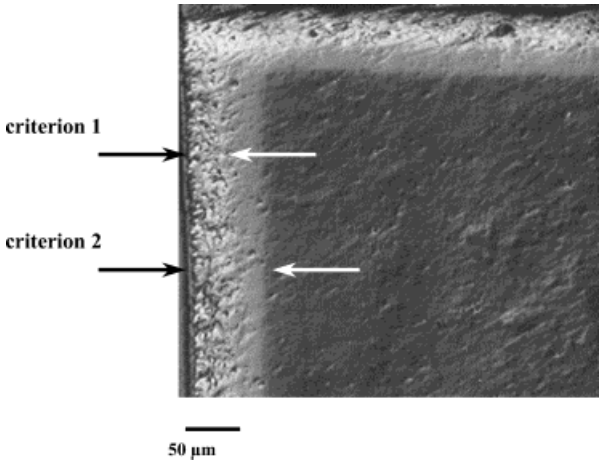

Figure 7 View by interferential contrast of a bulk polymer specimen after aging in air for 800 h at 240°C. Definition of two criteria.

Table III Experimental Data of Criteria 1 and 2 Measured by Means of Optical Microscopy

	Criterion 1 (μm)		Criterion 2 (μm)	
Aging Temperature (°C)	Experimental Values	Theoretical Values	Experimental Values	Theoretical Values
240	42 ± 11	35 ± 5	75 ± 6	72 ± 9
210	67 ± 11	65 ± 10	138 ± 13	137 ± 20
180	119 ± 9	115 ± 10	229 ± 29	241 ± 28

Note. Comparison with theoretical values computed from the kinetic model (2).

was extrapolated to the aging temperatures. The resulting profiles, $C(x)$, are presented in Figure 8.

From these, it is possible to determine the thickness profiles of oxidation rate, $r(C(x))$, mass loss, $[d(m/m_0)/dt]/(C(x))$, or oxidation products concentration, $Q(x) = \int_0^t r(x)dt$. These latter concentrations are shown in Figure 9.

Here, also, one can define two criteria corresponding, respectively, to the most oxidized superficial layer and to the whole oxidized layer (see Fig. 9). The stationary state values of predicted thicknesses of the oxidized layer can be compared to experimental ones in Table III. They agree surprisingly well.

A third possible way for checking the thickness oxidation profiles consists of computing mass loss rates of bulk specimens, from eqs. (24) and (27), and of comparing the stationary values with experimental ones determined by means of gravimetric experiments. For example, values obtained for a 1500-μm-thick specimen are reported in Table IV. As expected, theoretical results are in good agreement with experimental ones.

DISCUSSION

Up to now, proposed models were purely empirical, for instance, based on arbitrary reaction orders[9–11] or simply on power laws.[12–14] When oxygen diffusion is taken into account, it is only through questionable criteria.[14] As a consequence, these models are not able to predict the thickness oxidation profiles. More recently, a less

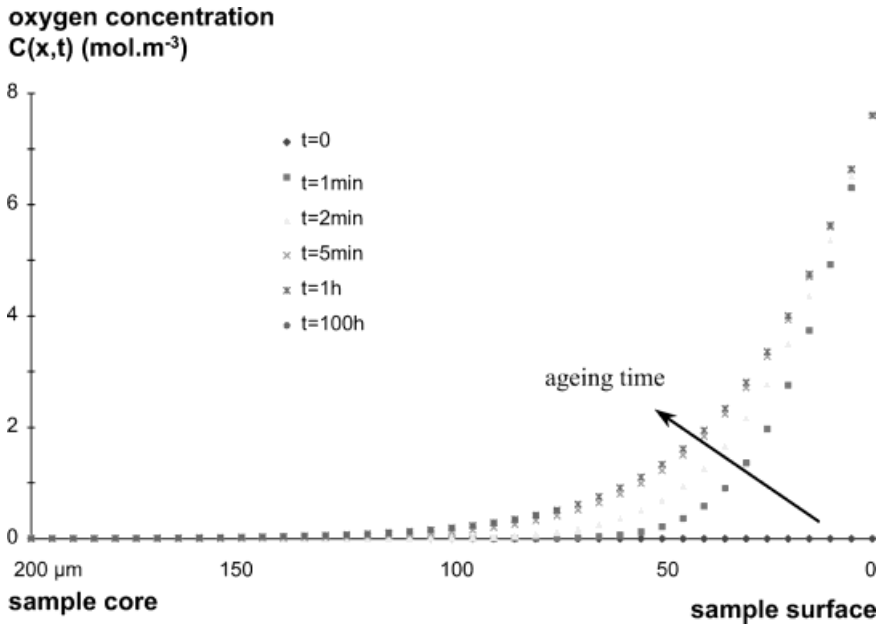

Figure 8 Profiles of O_2 concentration in air at 240°C. [Color figure can be viewed in the online issue, which is available at www.interscience.wiley.com.]

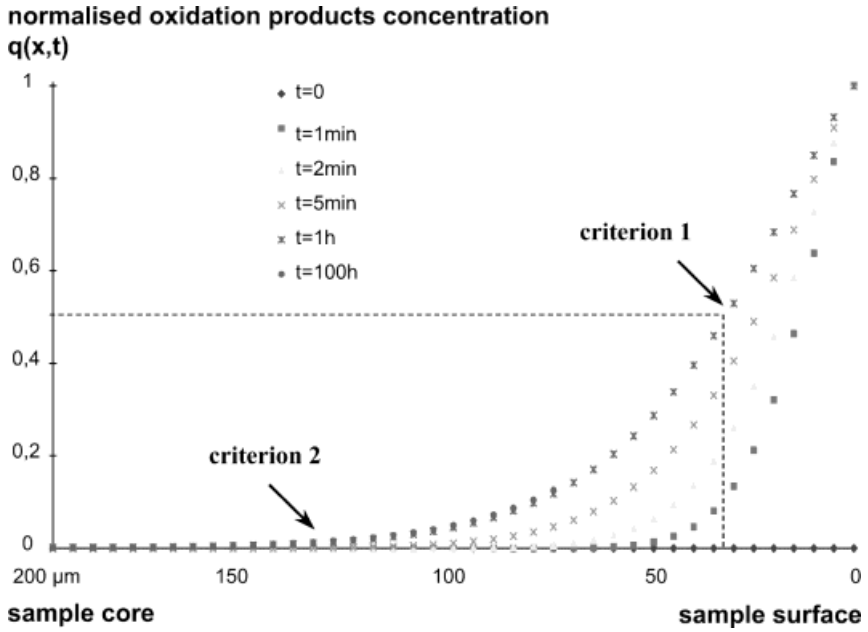

Figure 9 Profiles of oxidation products concentration in air at 240°C. [Color figure can be viewed in the online issue, which is available at www.interscience.wiley.com.]

empirical approach was proposed by Cunningham and McManus,[15] but the influence of O_2 concentration is not derived from a mechanistic scheme but from a more general theory of gas–solid reactions. Furthermore, this approach is focused on the case of progressed temperature experiments.

We dispose here of a nonempirical approach for the prediction of the thickness of the oxidized layer in thermally aged organic materials or composites. The model is based on three sets of experiments; one to determine the O_2 transport characteristics; solubility and diffusivity (from permeability tries); another to determine the critical sample thickness for O_2 diffusion control, based on a comparison of samples of different thicknesses; and the third, to determine the kinetics parameters, based on a study of the influence of O_2 pressure and temperature on aging rate. The predictive value of this approach is attested by the fact that, mixing independently determined chemical kinetic parameters and physical quantities [D in eq. (2)], one obtains a length value (the thickness of the oxidized layer) in excellent agreement with experimental data. The profile of oxidation products gives access to the density profile which, in turn, combined with the profile of mass loss gives access to the shrinkage profile, and then, to the stress profile if the mechanical behavior law of the material is known. A way is thus open for the nonempirical prediction of the oxidation-induced damage.

Table IV Maximum Weight Loss Rates Determined from Gravimetric Experiments Achieved on Bulk Samples 1500-μ-thick in Air at 240, 210, and 180°C (in the stationary state)

Aging Temperature (°C)	Maximum Weight Loss Rate (s^{-1})	
	Experimental Values	Theoretical Values
240	-3.9×10^{-8}	$-(3.5 \pm 1.5) \times 10^{-8}$
210	-1.4×10^{-8}	$-(1.4 \pm 0.5) \times 10^{-8}$
180	-2.1×10^{-9}	$-(4.4 \pm 1.6) \times 10^{-9}$

Note. Comparison with theoretical values computed from eqs. (24) and (27).

Indeed, it would be abusive to consider that the problem is completely resolved. First, the reported solution concerns only the stationary state with the (classical) implicit hypothesis that catastrophic damage occurs at very low conversion so that it is licit to assume that the substrate concentration ([PH]) is constant. A detailed examination of the kinetic curves of Figure 4 reveals, however, a positive curvature (the rate of mass loss slows down at long term). Because, at this stage, 10% or more of the mass has been lost, it is reasonable to suppose that the hypothesis of con-

stant substrate concentration is no longer valid. Then, we have to add to the kinetic scheme an equation describing the substrate consumption, for instance,

$$\frac{d[\mathrm{PH}]}{dt} = -\gamma k_1[\mathrm{PH}] - k_3[\mathrm{PO}_2^\circ][\mathrm{PH}] \qquad (5b)$$

where γ would be a stoichiometric parameter depending essentially on the exact yield of reactions Ib, Ic, and Id.

It is possible, then, to fit the experimental curves in their final part, as it will be shown in a future article. However, the possibility of solving the kinetic scheme (in stationary state) in an analytical way is lost; only numerical methods can be used.

Second, the stationary state hypothesis also ignores the initial part of the curves where mass varies nonmonotonically. Here, also, only numerical methods can be envisaged and the resolution needs the knowledge of at least two supplementary quantities: the initial hydroperoxide concentration $[\mathrm{POOH}]_0$ and the rate constant k_1 of hydroperoxide decomposition. The whole resolution of the kinetic scheme is in progress at the laboratory.

Considering eq. (2) (diffusion–reaction coupling), a question comes to mind: does oxidation modify O_2 solubility and diffusivity? In this case, D could not be considered a constant which would complicate as well the mathematical analysis as the experimental study. At this point in our knowledge, two cases can be distinguished:

(i) Before sample cracking, our results seem to indicate *a posteriori* that the hypothesis of constant D and S values was justified.
(ii) From a panoramic overview of structure–property relationships in this field,[16] it seems that no big variation of D and S is to be expected as long as oxidation does not induce strong variations of the polymer polarity or change of physical state (from glassy to rubbery state, for instance). Important variations of the polymer polarity can be eventually expected in initially apolar polymers, for instance, polyolefines, but not in initially polar polymers such as bismaleimide.

CONCLUSION

To minimize the risks of lifetime prediction for oxidative aging of bismaleimide networks and the corresponding composites, the suppression of most of the empirical steps by using a model based on a standard mechanistic scheme of branched radical oxidation is proposed. The advantage of this approach is that it offers in principle a possibility of independent checking at every elementary step. The basic principle is to determine the thickness distribution of oxidation products from an equation coupling O_2 diffusion and its consumption rate:

$$\frac{\partial C}{\partial t} = D\,\frac{\partial^2 C}{\partial x^2} - r(C)$$

The diffusion constant, D, and the equilibrium concentration, C_S, are determined from permeability measurements.

$r(C)$ is determined from the mechanistic scheme and the parameter values are determined from experiments done on thin samples at various O_2 pressures. A simple but reasonable hypothesis (mass loss occurs only in initiation step) allows the establishment of a nonempirical link between the O_2 consumption rate and the mass loss rate (in stationary state).

Experiments made on samples of different thicknesses from 50 to 1500 μm, or on bulk samples, allow the determination of the thickness of the oxidized layer. Experimental results are in excellent agreement with model predictions.

The authors acknowledge J. M. Rey (CEA Saclay) for helpful permeation experiments and Aerospatiale-Matra (CCR Suresnes) for supplying neat resin materials.

REFERENCES

1. Audouin, L.; Gueguen, V.; Tchakhtchi, A.; Verdu, J. J Polym Sci, Polym Chem Ed 1995, 33, 921.
2. Audouin, L.; Langlois, V.; Verdu, J.; De Bruijn, J. C. M. J Mater Sci 1994, 29, 569.
3. Favre, J.-P.; Levadoux, H.; Ochin, T.; Cinquin, J. 10th Natl. Conf. on Comp. Mat. (JNC-10); (Baptiste, D.; Vautrin, A., Eds.), 1996, 1, 205.
4. Didier, S.; Rey, J. M.; Pailler, P.; Bunsell, A. R. Cryogenics 1998, 38, 135.
5. Gugumus, F. Polym Degrad Stab 1995, 49, 29.
6. Gillen, K. T.; Wise, J.; Clough, R. L. Polym Degrad Stab 1995, 47, 149.
7. Verdu, J. Macromol Symp 1997, 115, 116.
8. Matisova-Rychla, L.; Rychly, J.; Verdu, J.; Audouin, L.; Csomorova, K. Polym Degrad Stab 1995, 19, 51.

9. Hinkley, J. A.; Nelson, J. B. J Adv Mater 1994, 45.
10. Reignier, N.; Mortaigne, B. Polym Adv Technol 1994, 5, 513.
11. Reignier, N.; Autran, M.; Chevallier, D.; Mortaigne, B. 11th Natl. Conf. on Comp. Mat. (JNC-11); (Lamon, J.; Baptiste, D., Eds.), 1997, 1, 217.
12. Nelson, J. B. ASTM STP-813 (O'Brien, T. K., Ed.), 1983, 206.
13. Bowles, K. J.; Nowak, G. J Comp Mater 1988, 22(6), 966.
14. Nam, J. D.; Seferis, J. C. SAMPE Qrtly 1992, 24(1), 10.
15. Cunningham, R. A.; McManus, H. L. Proc. ASME Aerospace Division, ASME 1996, 52, 353.
16. Van Krevelen, D. W.; Hoftyzer, P. J. Properties of Polymers. Their estimation and correlation with chemical structure, Amsterdam: Elsevier, 1976; Chapter 18, p. 535.